Received: 9 April 2020 | Revised: 3 November 2020 | Accepted: 5 November 2020

DOI: 10.1002/app.50287

ARTICLE

Applied Polymer SCIENCE WILEY

Biocomposite scaffolds for 3D cell culture: Propolis enriched polyvinyl alcohol nanofibers favoring cell adhesion

Rumeysa Bilginer[1] | **Dilce Ozkendir-Inanc**[2] | **Umit Hakan Yildiz**[3] | **Ahu Arslan-Yildiz**[1]

[1]Department of Bioengineering, Izmir Institute of Technology (IZTECH), Izmir, Turkey

[2]Department of Photonic, Izmir Institute of Technology (IZTECH), Izmir, Turkey

[3]Department of Chemistry, Izmir Institute of Technology (IZTECH), Izmir, Turkey

Correspondence
Ahu Arslan-Yildiz, Izmir Institute of Technology, Department of Bioengineering, 35430, Izmir, Turkey.
Email: ahuarslan@iyte.edu.tr

Abstract

The objective of this work is generation of propolis/polyvinyl alcohol (PVA) scaffold by electrospinning for 3D cell culture. Here, PVA used as co-spinning agent since propolis alone cannot be easily processed by electrospinning methodology. Propolis takes charge in maximizing biological aspect of scaffold to facilitate cell attachment and proliferation. Morphological analysis showed size of the electrospun nanofibers varied between 172–523 nm and 345–687 nm in diameter, for non-crosslinked and crosslinked scaffolds, respectively. Incorporation of propolis resulted in desired surface properties of hybrid matrix, where hybrid scaffolds highly favored protein adsorption. To examine cell compatibility, NIH-3T3 and HeLa cells were seeded on propolis/PVA hybrid scaffold. Results confirmed that integration of propolis supported cell adhesion and cell proliferation. Also, results indicated electrospun propolis/PVA hybrid scaffold provide suitable microenvironment for cell culturing. Therefore, developed hybrid scaffold could be considered as potential candidate for 3D cell culture and tissue engineering.

KEYWORDS

3D cell culture, biomimetic, co-electrospinning, propolis, tissue engineering

1 | INTRODUCTION

Native tissue microenvironments are formed by complex 3D fibrillar network of extracellular matrix (ECM), which can be mimicked at the micro- and nano-scale by electrospinning.[1–3] The electrospun scaffolds can be fabricated directly from synthetic and natural polymers[4]. However, both synthetic and natural polymers exhibit drawbacks during electrospinning process; while synthetic polymers limit cellular interactions and biocompatibility, natural ones have obstacles such as high viscosity or difficulty in gelling.[5,6] Therefore, recent efforts have been focused on construction of hybrid scaffolds via integration of natural polymers into synthetic ones to eliminate undesired properties.[4,7–9] Integration of natural material into synthetic scaffold favors cell proliferation, cell–cell, and cell-scaffold interaction, and also it paves the way to mimic ECM microenvironment.[10–15] Most of those studies focusing on integration of ECM components such as collagen,[3,16,17] hyaluronic acid,[18] or other natural polymers like elastin,[16,19,20] silk fibroin[21] into synthetic polymers via electrospinning, since electrospun natural materials provide ECM-like structure while supporting bioactivity.

Propolis (P) is a promising natural material to augment bioactivity of the scaffold in a cost-effective way. It

consist of 50% resin, 30% wax, 10% essential and aromatic oils and finally 5% pollen and other compounds.[22] Besides, propolis has antibacterial, antifungal and antioxidant properties due to the presence of phenolic compound, terpenoid and alkaloids.[23] There are varied studies that report cell viability in the presence of propolis, which indicate biocompatible and toxic-free nature of propolis.[24,25] Antibacterial property of propolis can be advantageous, especially for tissue-engineering and regenerative medicine applications, to prevent host from infection after implantation process. These properties make propolis a potential candidate as a scaffold for tissue engineering.

In this article, potential of propolis enriched polyvinyl alcohol (PVA) was evaluated as a tissue-engineering scaffold. Propolis/PVA nanofiber hybrid scaffolds were fabricated through electrospining based on co-spinning approach[26] where propolis was easily processed with the aid of PVA. To date, varied synthetic polymers, including PVA, have been employed as a tissue engineering scaffold.[18,27–34] PVA is widely used in pharmaceutical and biotechnology applications[35–38] owing to its solubility in water. Also, mechanical features and high-water uptake capacity of PVA assist to simulate living tissue when incorporated with biologically active substitutes.[39] Hence, PVA has been integrated mostly with natural polymers to ameliorate its biological activity.[40] To the best of our knowledge, no one has reported utilization of propolis enriched PVA as a tissue-engineering scaffold. PVA was used as nontoxic supporting material of propolis to be integrated in, and propolis was employed to serve as quasi-ECM component that fosters cell attachment and cell proliferation. The characterization of electrospun hybrid propolis/PVA scaffold was carried out with SEM, ATR-FTIR, AFM, contact angle, and protein adsorption analysis. Cellular compatibility was evaluated through cell proliferation, cell viability, and cell adhesion of NIH-3T3 and Hela cell lines on propolis/PVA scaffold.

2 | EXPERIMENTAL

Ethanolic extract of purified propolis was purchased from a local distributor (Ekobio Co. Ltd., Izmir, Turkey). Polyvinyl alcohol (PVA, wt 30,000–70,000), bovine serum albumin (BSA) as lyophilized powder, glutaraldehyde (GTA) was purchased from Sigma Aldrich. Ethanol (99%) and hydrochloric acid (HCl) (37%) purchased from Isolab. Sodium dodecyl sulfate (SDS) was purchased from Bioshop. NIH-3T3 mouse fibroblast cell line (ATCC CRL-1658), HeLa human cervical cancer cell line (ATCC CCL-2) high-glucose dulbecco's modified eagle's medium (DMEM), penicillin–streptomycin (P/S), trypsin–EDTA solution (0.25%, sterile-filtered, BioReagent), fetal bovine serum (FBS-Gibco), phosphate buffer saline (PBS, pH 7.4 10X, Gibco), Resazurin sodium salt (ChemCruz) were used for cell culture studies.

2.1 | Fabrication of electrospun propolis/PVA scaffolds

Pristine PVA (20%) and 5, 10, 15, and 20% propolis enriched PVA scaffolds were fabricated by coelectrospinning (Inovenso, Ne300) methodology as explained elsewhere.[26] 20% (wt/vol) PVA solution was dissolved in deionized water and stirred overnight at room temperature. Ethanol solubilized propolis solutions were added to PVA solution. Later, propolis and PVA solution were blended and mixed with magnetic stirrer for 2–3 h prior to electrospinning. Then, electrospinning of pristine PVA was performed at room temperature with 28 kV, 1 ml/h flow rate and 180 mm distance to collector, without rotating. On the other hand, propolis/PVA co-spinning was accomplished at 24 kV voltage, 1 ml/h flow rate, 400 rpm and 180 mm distance to collector. The electrospun hybrid nanofibers were gathered on collector, which was covered by aluminum sheet. Since PVA is a water-soluble polymer, pristine PVA and propolis enriched PVA scaffolds were crosslinked before 3D cell culture experiments. Electrospun scaffolds were exposed to crosslinking solution containing 0.01 M GTA in acetone and HCl, which were followed by rinsing with PBS and drying of propolis/PVA mats in fume hood for further studies.

2.2 | Characterization of propolis/PVA scaffolds

Surface morphologies of crosslinked and non-crosslinked scaffolds were observed by scanning electron microscope (SEM-Quanta FEG 250) analysis. The samples were fixed and coated with thin gold layer (Emitech K550X) under argon atmosphere prior to SEM analysis. Average diameter was calculated from approximately around 100 nanofibers through Image J software (NIH). Surface topography and mechanical properties of propolis/PVA scaffolds were measured using Nanosurf CoreAFM (Switzerland). Electrospun propolis/PVA nanofibers, both crosslinked and non-crosslinked, were placed on microscope slide and AFM analysis was accomplished with beam shaped cantilever in contact mode (Stad 0.2 LAuD, NanoAndMore GMBH, Germany) having a nominal spring constant of 0.2 N/m and tip radius of 7 nm. 512 lines at a speed of 1 s per line and 50 nN set point were acquired for each image. Surface roughness and Young's modulus values were calculated using AFM data

analysis. Atomic J was used during mapping of data collected from Young's modulus measurements and analyzed with Origin Pro 2016. A series with 256 force-distance curves was calculated for $25 \times 25\ \mu m^2$ regions and fit up to 1 μm tip deflections with a Hertz (sphere) model. Presence of the propolis was confirmed through spectrophotometric analysis where non-crosslinked propolis/PVA scaffolds were solubilized and absorbance characteristics were evaluated. Prior to analysis, propolis/PVA mats were dissolved in ethanol: water (1:1) mixture and stirred overnight. Absorbance scan (200–800 nm) was obtained for individual samples using UV–Vis spectrophotometer (Shimadzu UV 2550) at room temperature. Presence of propolis and crosslinking efficiency were evaluated through both ATR-FTIR and wettability analysis. Crosslinked and non-crosslinked Propolis/PVA samples were analyzed by FTIR in ATR mode (Perkin Elmer-diamond/ZnSe crystal). Obtained data was plotted by OriginPro (Northampton, MA) software. Wettability testing was performed on non-crosslinked and crosslinked propolis/PVA scaffolds via contact angle analysis (Attension) at static mode. Three individual samples were used for each measurement and average contact angle values were determined for each scaffold.

2.3 | Use of propolis/PVA scaffolds for 3D cell culture

Bicinchoninic acid (BCA) assay kit (PierceTM, Thermo Scientific) was used to investigate protein adsorption capacity of each scaffold. Triple replicate from each scaffold were analyzed against BSA solutions varying between 25–2000 μg/ml. Three individual replicates were incubated in BSA solutions and the adsorbed protein on the scaffolds were rinsed by incubating with 5% (wt/vol) SDS for 1 h. Absorbance values were obtained using micro plate reader (Fisher Scientific accuSkan GO UV/Vis Spectrophotometer) at 562 nm and data was processed using Origin Pro (Northampton, MA) software.

NIH-3T3 mouse fibroblast and HeLa human cervical cancer cells were cultured in standard medium (DMEM, Gibco) containing 10% FBS (Gibco) and 1% penicillin/streptomycin. Cells were incubated under 5% CO_2 at 37°C. Prior to cell seeding, scaffolds were sterilized for 30 min under UV light. 1 x 10^5 number of cells from each cell line was seeded separately on crosslinked propolis/PVA scaffolds as three replicates. Cell proliferation and toxicity profiles were evaluated via Alamar Blue assay for 7 days period. Cell cultured scaffolds for day 1, 3, 5, and 7, were rinsed with PBS and incubated in 1% resazurin sodium salt solution for 4 h. Cell proliferation profiles on crosslinked propolis/PVA scaffolds were assessed through absorbance values at 570 and 600 nm.

In order to visualize cells and analyze the cell morphology and behavior on propolis/PVA scaffolds, SEM analysis was used. Cell cultured propolis/PVA scaffolds for day 1 and 7 were fixed with 4% paraformaldehyde and rinsed with PBS, and then were analyzed after drying at room temperature. Anti-collagen Type I-FITC (Sigma-Aldrich) was applied for 80 min at room temperature for immunostaining of Collagen Type I. Cell spreading analysis was done via Image J software through image analysis of SEM data where at least three independent experimental results were analyzed (n = 3).

2.4 | Statistics

Cell viability and proliferation experiments were done as six independent replicates and data was expressed as mean ± SD. Two-way ANOVA followed by Tukey test for multiple comparison was performed by GraphPad Prism software to determine significant differences between mean values of experimental groups. Statistical significance between groups was considered at $p < 0.05$.

3 | RESULT AND DISCUSSION

To increase the bioactivity of PVA-based scaffold, propolis was introduced into PVA scaffold by co-spinning approach. As depicted in Figure 1, PVA was utilized to accumulate propolis in scaffold because of PVA's nontoxic nature, and it was used as co-spinning agent. Propolis was used to increase bioactivity of scaffold in terms of cell–cell and cell-matrix interaction. Propolis/PVA scaffolds were characterized by SEM, UV–Vis, ATR-FTIR, water contact angle, AFM, and protein adsorption analyses. For in vitro studies, cell proliferation and adhesion on propolis/PVA scaffolds were carried out with NIH-3T3, HeLa, MDA-MB-231, and SH-SY5Y cell lines to demonstrate its potential to be used as scaffold and disease model for drug screening studies.

3.1 | Evaluation of propolis/PVA scaffold morphology

In this study, pristine PVA scaffold and Propolis/PVA scaffolds containing 5–20% propolis were fabricated through electrospinning technique. Since PVA is a water-soluble polymer, crosslinking of each scaffold was done with 0.01 M GTA solution in order to achieve water-resistant nanofiber scaffolds. As given in Figure 2, SEM analysis of propolis/PVA fiber morphology revealed that homogenous, bead-free nanofiber

mats were obtained successfully before and after crosslinking. As observed by SEM analysis, both propolis addition and crosslinking process contributes to the increase of fiber diameters. The diameter of PVA fibers has slightly increased due to propolis coverage. Diameter of PVA fibers was increased up to 523 nm ±144.67 with propolis addition, while pristine PVA has an average diameter of 172.11 nm ± 62.12 before crosslinking. At the same time, fiber diameter of propolis/PVA scaffolds was also increased due to crosslinking process, provided by Figure 2.

This significant increment in fiber diameter as propolis added can be attributed to effect of increased viscosity, adhesive properties and repulsive force of propolis.[41,42] Upon crosslinking, combination of fibers occurs due to functional substituent groups provided by propolis content, where -OH groups in PVA react with both propolis and neighboring PVA, result in densely packing of fibers due to conglutination. When the SEM images of propolis added PVA fibers are closely examined (given by inset images), regardless of propolis amount, fine, and smooth fibers are obtained. As a result, crosslinking and addition of propolis increased diameter of scaffolds which lead to diminish of surface area.[43] This signifies that scaffold morphology can be tuned by incorporation of natural polymers in synthetic ones.

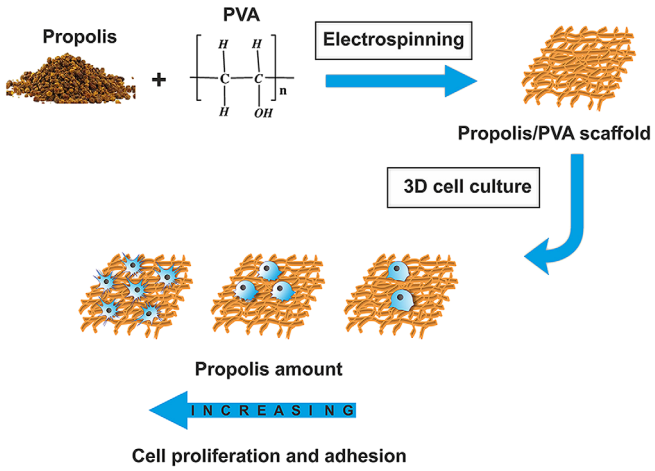

FIGURE 1 Schematic representation of propolis/PVA hybrid scaffold fabrication and utilization in 3D cell culture. PVA, polyvinyl alcohol [Color figure can be viewed at wileyonlinelibrary.com]

3.2 | Surface topography and mechanical testing of propolis/PVA scaffolds via AFM

Figure 3 illustrates the topography image of non-crosslinked and crosslinked PVA in varying propolis

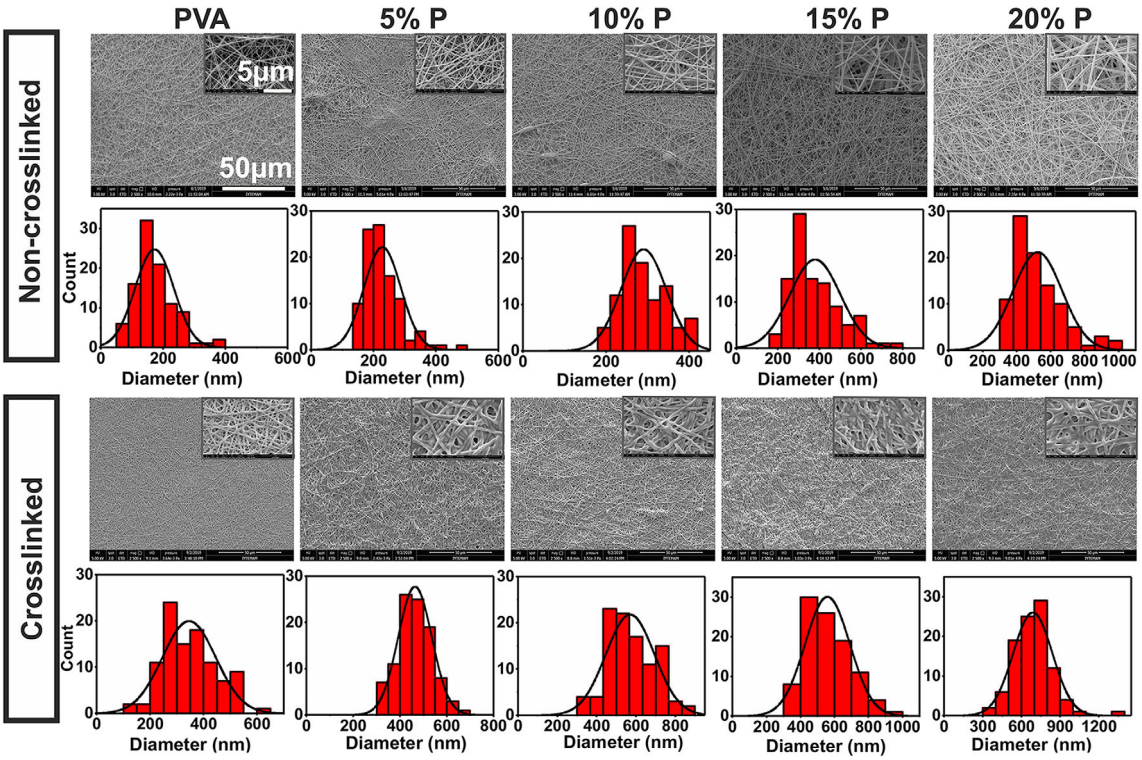

FIGURE 2 SEM images and diameter distribution of non-crosslinked and crosslinked propolis/PVA scaffolds for 0, 5, 10, 15, and 20% propolis content. PVA, polyvinyl alcohol; SEM, scanning electron microscope [Color figure can be viewed at wileyonlinelibrary.com]

concentrations. Young's modulus mapping of crosslinked PVA and force-distance curves have been also shown in Figure 3. The fiber structures are obvious both in crosslinked and non-crosslinked samples. Surface topography revealed that fibers were smoother by crosslinking; the PVA polymers exhibited less surface roughness as compared to non-crosslinked even at higher propolis concentrations. The total roughness of crosslinked PVA samples were determined as 418 nm referring to 50% decrease as compared to non-crosslinked fibers. It was obviously known that chemical crosslinking tends to dramatically decrease the surface roughness due to the detrimental effect on the polymer chains.[44,45] In addition, crosslinking causes a dramatic increase in stiffness of the PVA fibers, and this Young's modulus mapping for crosslinked PVA in varying propolis concentration was

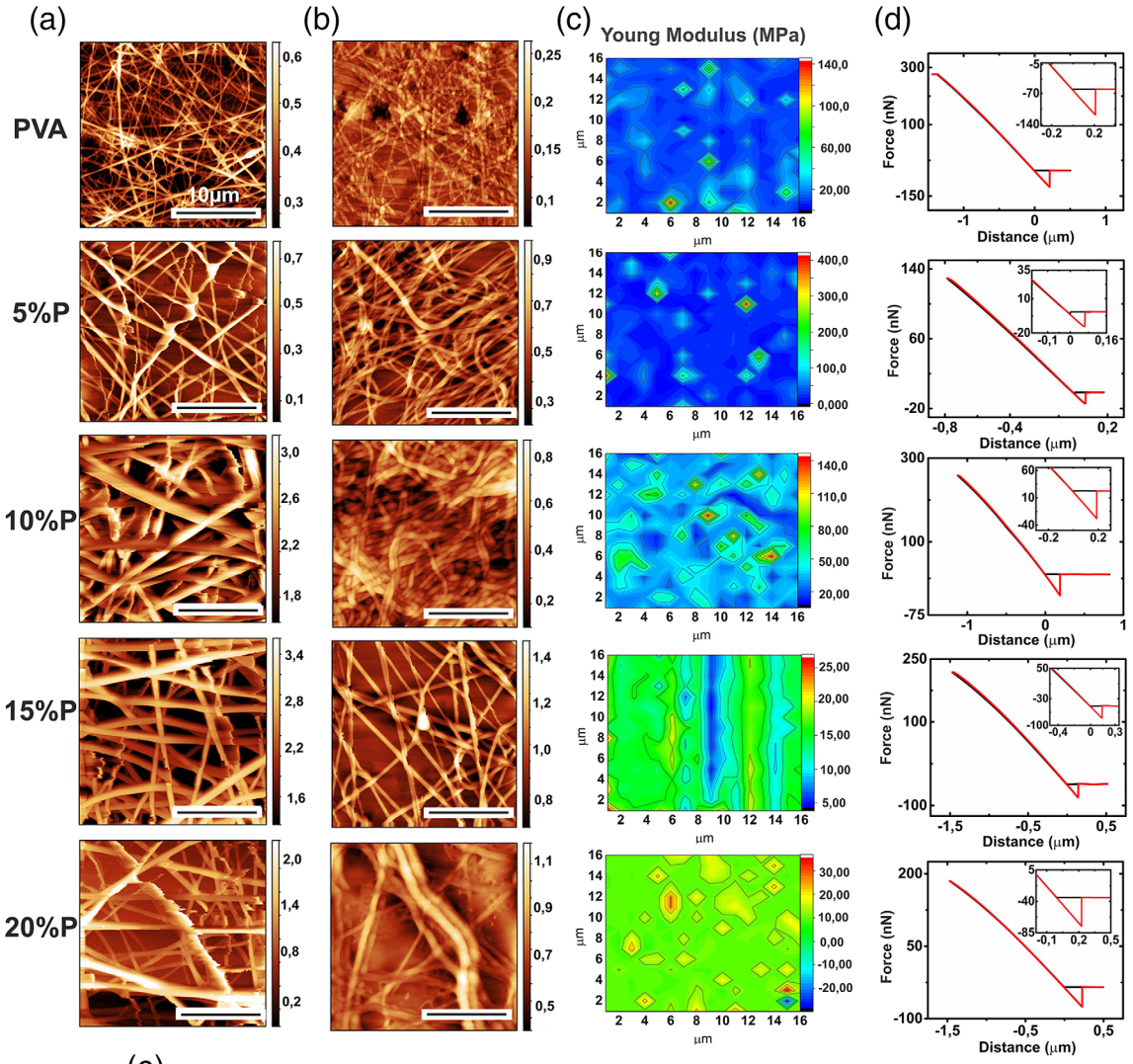

(e)

Propolis Concentration (%)	Average Young Modulus (MPa)	
	Non-crosslinked	Crosslinked
PVA	21,75 ± 8,44	13,81 ± 7,72
5%P	21,19 ± 6,43	24,33 ± 9,83
10%P	46,99 ± 19,35	35,71 ± 13,96
15%P	14,55 ± 5,69	14,02 ± 3,21
20%P	6,66 ± 2,73	10,91 ± 4,57

FIGURE 3 AFM topography image of (a) non-crosslinked (b) crosslinked (c) Young's modulus map of crosslinked and (d) force-distance analysis of crosslinked PVA nanofibers with 0, 5, 10, 15, and 20% propolis concentrations (e) average young modulus of propolis/PVA scaffolds. PVA, polyvinyl alcohol [Color figure can be viewed at wileyonlinelibrary.com]

shown in Figure 3(c). Young's modulus values were varied for each concentration, but as the concentration increases, the distribution of Young's modulus on the surface became homogeneous. An increase in Young modulus values was observed up to 10% propolis concentration, above this concentration, significant decrease in Young modulus was observed. This can be attributed to deteriorated chain alignments and chain packing due to hindrance of PVA chains by propolis.[42] Although higher propolis concentration (>10%) causes lower stiffness, homogeneity of Young's modulus maps of 15 and 20% propolis samples are notable. The uniform mechanical property at higher propolis concentration may be due to the easy intermixing of propolis with PVA thereby forming homogeneous hybrid Propolis/PVA. The pull-off force for each sample was determined by force-distance analysis as shown in Figure 3(d). While the amount of propolis concentration increases, the average pull-off force decreases up to 10% propolis concentration (5.85 nN). After 10% propolis concentration, the pull-off force recorded as 41 nN. Furthermore, crosslinking increased the stiffness, and caused a reduction in the adhesion of propolis on the PVA surface.[44]

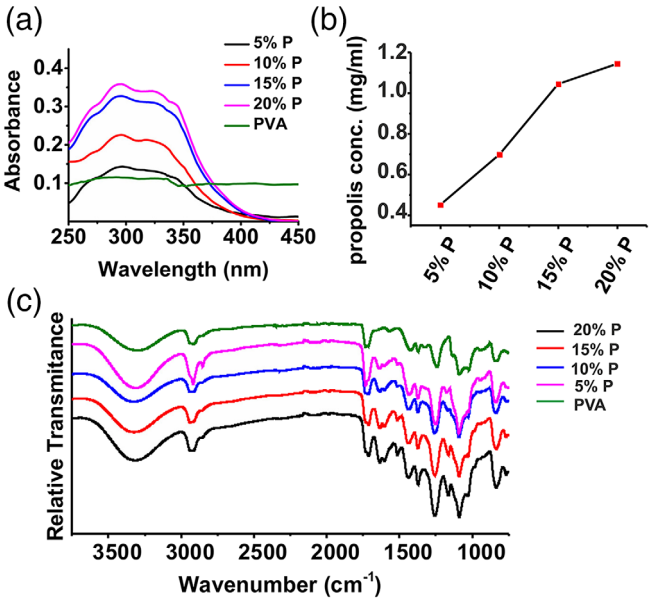

FIGURE 4 (a) UV–Vis spectrum (b) propolis concentration (at 310 nm) and (c) ATR-FTIR analysis of 0, 5, 10, 15, and 20% propolis/PVA scaffolds. PVA, polyvinyl alcohol [Color figure can be viewed at wileyonlinelibrary.com]

3.3 | Validation of propolis presence in propolis/PVA scaffolds

Electrospun propolis/PVA nanofibrous scaffolds were investigated via absorbance spectroscopy and ATR-FTIR analysis to confirm the presence of propolis. The concentration of propolis and content of propolis/PVA scaffolds were analyzed. As reported in literature,[46] propolis exhibits an absorption maximum in the range of 280–330 nm due to its phenolic content. Figure 4(a) represents absorbance spectrum of hybrid propolis/PVA scaffolds, where propolis containing hybrid scaffolds has characteristic absorbance maxima at around 310 nm while pristine PVA scaffold does not have significant absorbance. Final propolis concentration in hybrid scaffolds was calculated through absorbance spectroscopy where standard curve of propolis ranging between 25 and 2000 μg/ml. The maximum propolis concentration in electrospun hybrid scaffold was 1.143 mg/ml for 20% propolis/PVA scaffold. Given in Figure 4(a),(b), the absorbance value proportionally increased demonstrating that concentration of propolis increased. Results clearly showed the presence and concentration of propolis in electrospun hybrid scaffolds.

ATR-FTIR analysis was done to analyze chemical content of hybrid scaffolds and to investigate presence of propolis in hybrid nanofibers. FTIR spectrum of pristine PVA and hybrid propolis/PVA scaffolds were given in Figure 4(c). Absorption bands between 3500 and 3050 cm^{-1} indicate OH groups of PVA and phenolic compounds of propolis. 3400–3200 cm^{-1} bands may also indicate presence of amino acids in propolis. In addition, 2920 cm^{-1} confirms presence of polyphenols and ester groups, while 1085 and 830 cm^{-1} correspond to the stretching of aromatic ether C—O and angular deformation of C—H respectively.[47] 1160–1250 cm^{-1} was sign of amide and amide compounds in propolis. 1608 and 1648 cm^{-1} bands were indications of C═O, C═C and asymmetric bending of N—H showing flavonoids and amino acid existence in propolis.[46,48]

3.4 | Surface wettability analysis

Hydrophilicity is a paramount phenomenon that effects performance of cell-matrix interaction, cell proliferation and spreading.[49] Wettability of propolis/PVA scaffolds was analyzed through water contact angle by sessile drop method (Figure 5(a)). Pristine PVA shows high hydrophilicity (10.51 ± 4.43) owing to its water-soluble characteristics. Prior to crosslinking, contact angle was increased via integration of propolis into the scaffold up to 44.20 ± 5.07 with 20% propolis addition. Contact angle of non-crosslinked pristine PVA and propolis/PVA hybrid scaffolds were proportionally increased with increasing amount of propolis, as well. Whereas pristine PVA has a contact angle of 59.68 ± 13.28, it was increased to 84.82 ± 8.88 for 20% propolis containing hybrid scaffolds. As a

result, propolis/PVA hybrid scaffolds showed moderate hydrophilic character, which supports cell attachment compared to super hydrophilic or hydrophobic surfaces,[50] as well confirming GTA can be sufficient for fine-tuning of wettability.

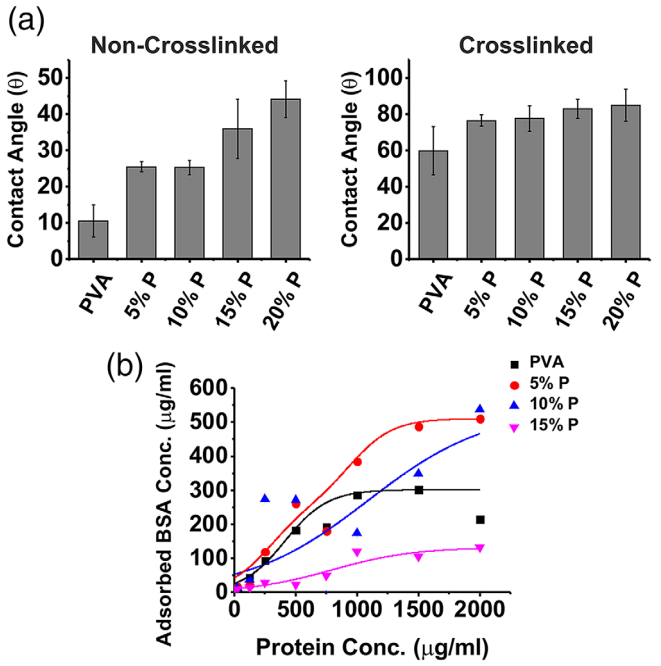

FIGURE 5 (a) Representative contact angle curves of non-crosslinked and crosslinked propolis/PVA scaffolds (b) protein adsorption profiles of propolis/PVA scaffolds (n = 3). PVA, polyvinyl alcohol [Color figure can be viewed at wileyonlinelibrary.com]

3.5 | Protein adsorption assessment of propolis/PVA scaffolds

Protein adsorption analysis is an important technique to evaluate cell-matrix interaction prior to cellular studies. Protein adsorption profiles (Figure 5(b)) of propolis/PVA hybrid scaffolds were investigated via BCA assay. All hybrid scaffolds reached at equilibrium at total protein concentration of 1500 μg/ml. The highest amount of adsorbed protein, at around 500 μg/ml, was obtained for both 5 and 10% propolis/PVA scaffolds. However, higher propolis containing hybrid scaffolds had lower protein adsorption capacity, which can be attributed to amino acid or protein content of propolis. Overall, protein adsorption profiles show that propolis/PVA scaffolds has a certain protein-holding capacity that can favor cell-scaffold interaction.

3.6 | In vitro 3D cell culture studies

Cytocompatibility of propolis enriched hybrid scaffolds were investigated through cell viability and proliferation analyses. Therefore, NIH-3T3 and HeLa cell lines were cultured on propolis/PVA scaffolds for 1 week to investigate cell viability and proliferation behaviors, and they were monitored through Alamar Blue assay. Here, pristine PVA was used as a 3D control for comparison. At the beginning cells were proliferated on pristine PVA dramatically, however, cell attachment decreased in long term indicating PVA was not compatible as much as propolis/PVA scaffolds (Figure 6(a)). Propolis/PVA

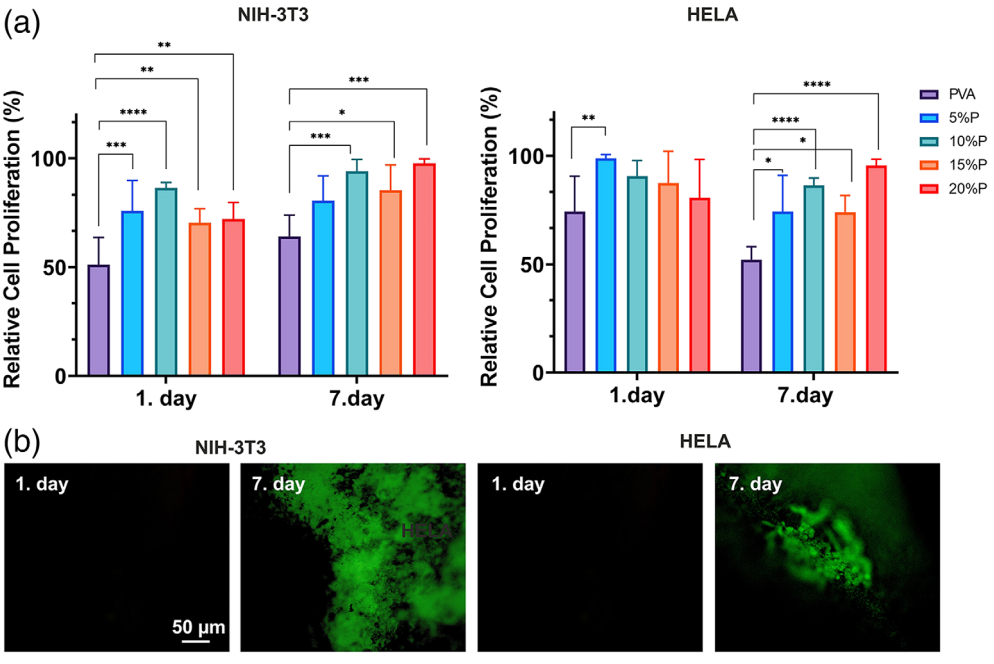

FIGURE 6 (a) Cytotoxicity and proliferation analysis of NIH-3T3 and HeLa cells for 1 and 7 days of culture (n = 6) (statistical difference: *$p < 0.05$, **$p < 0.01$, ***$p < 0.001$, ****$p < 0.0001$). (b) Immunofluorescence staining of collagen Type-1 for 3D cultured NIH-3T3 and HeLa cells on propolis/PVA scaffold. PVA, polyvinyl alcohol [Color figure can be viewed at wileyonlinelibrary.com]

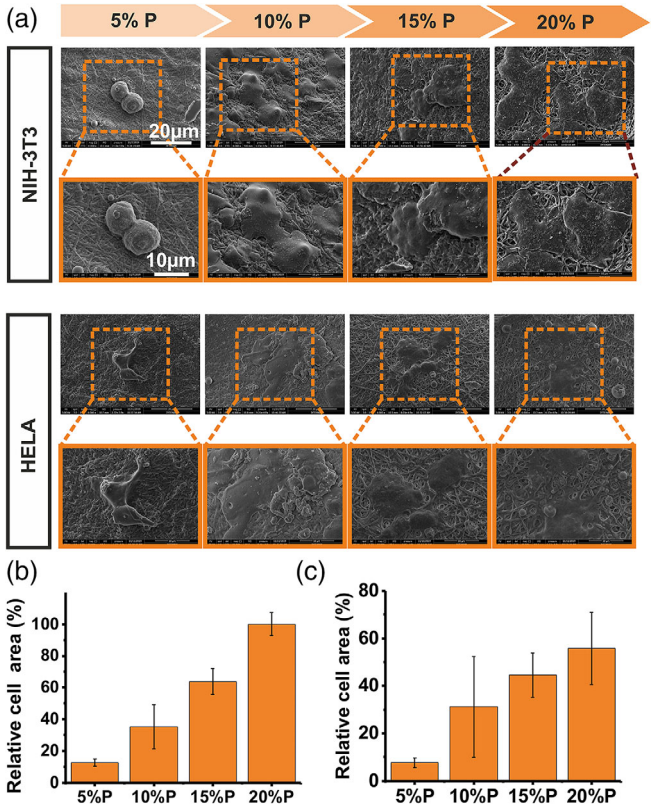

FIGURE 7 (a) SEM images for NIH-3T3 and HeLa cell adhesion profiles on propolis/PVA hybrid scaffolds for 7 days culture. Relative cell area distribution of (b) NIH-3T3 cells and (c) HeLa cells, on propolis/PVA scaffold. PVA, polyvinyl alcohol [Color figure can be viewed at wileyonlinelibrary.com]

scaffold shows statistically higher proliferation rate compared to PVA. After 7-day culture, 20P performed much better than others for both cell lines in terms of cell proliferation, and there is significant difference between 20P and PVA scaffold. In parallel, to confirm the formation of ECM Collagen Type-1 immunostaining was done (Figure 6(b)). ECM formation and Collagen secretion was observed by positive staining of Collagen Type-1 on day 7 for both NIH-3T3 and HeLa cell lines.

Moreover, cell attachment and morphology of NIH-3T3 and HELA cells on propolis/PVA scaffolds were monitored for one-week period as shown in Figure 7. Cells were adhered as round shape on 5% propolis/PVA. Cell number and spreading area have been enhanced and correlated with the increasing propolis content (Figure 7(b),(c)), which overlap with cell proliferation result as well. For each hybrid scaffold containing varied propolis amount, cells contacted neighboring cells. However, cells on hybrid scaffolds with a higher propolis content spread more and flattened indicating favored cell attachment and cell-matrix interaction. The cell proliferation accelerated with propolis enhancement, which means propolis might have a synergic effect on cell attachment and proliferation. The possible reason of this, as propolis consist of biological components, it provides recognition elements more than pristine PVA.[51] The result clearly demonstrated that propolis exhibited biocompatible properties. Propolis enriched hybrid scaffold could model microenvironment of ECM and could be a potential candidate for 3D cell culture studies.

4 | CONCLUSION

Propolis is a biocompatible and bioactive natural substance, which has a great potential to serve as a scaffold component. In this study, electrospun Propolis/PVA hybrid scaffold was used to generate biocompatible and biofunctional microenvironment for 3D cell culture. PVA nanofiber scaffolds with 5, 10, 15, and 20% propolis content were successfully fabricated using electrospinning method. Scaffolds were crosslinked with GTA to gain water-resistance for cell culture studies. Protein adsorption studies proved that propolis enriched scaffolds have a good protein holding capacity which facilitates cell attachment as well. Propolis/PVA hybrid scaffolds were utilized to culture several cell lines confirming that integration of propolis improved biocompatibility of PVA and supported cell growth. It was also observed that cells could attach and spread more on hybrid scaffold with an increasing amount of propolis. Overall, obtained results indicated that propolis enriched hybrid scaffolds showed better properties compared to pristine PVA. Therefore, it is a promising bioactive scaffold mimicking 3D microenvironment of ECM and can be implemented as a scaffold for 3D cell culture and tissue engineering applications.

ACKNOWLEDGMENTS

The authors acknowledge Izmir Institute of Technology Biotechnology and Bioengineering Research and Application Center for the instrumental facilities provided to accomplish this work.

ORCID

Ahu Arslan-Yildiz https://orcid.org/0000-0003-0348-0575

REFERENCES

[1] Z.-M. Huang, Y. Z. Zhang, M. Kotaki, S. Ramakrishna, *Compos. Sci. Technol.* **2003**, *63*, 2223.
[2] R. Vasita, D. S. Katti, *Int. J. Nanomed.* **2006**, *1*, 15.

[3] E. Turker, U. H. Yildiz, A. Arslan Yildiz, *Int. J. Biol. Macromol.* **2019**, *139*, 1054.
[4] R. N. Oliveira, G. B. McGuinness, R. Rouze, B. Quilty, P. Cahill, G. D. A. Soares, R. M. S. M. Thiré, *J. Appl. Polym. Sci.* **2015**, *132*, 42129.
[5] D. P. Bhattarai, L. E. Aguilar, C. H. Park, C. S. Kim, *Membranes* **2018**, *8*, 62.
[6] E. Mele, *J. Mater. Chem. B* **2016**, *4*, 4801.
[7] M. Setayeshmehr, E. Esfandiari, B. Hashemibeni, A. H. Tavakoli, M. Rafienia, A. Samadikuchaksaraei, L. Moroni, M. T. Joghataei, *Eur. Polym. J.* **2019**, *118*, 528.
[8] M. Setayeshmehr, E. Esfandiari, M. Rafieinia, B. Hashemibeni, A. Taheri-Kafrani, A. Samadikuchaksaraei, L. David, L. M. Kaplan, M. T. Joghataei, *Tissue Eng., Part B* **2019**, *25*, 202.
[9] P. A. Ulloa, J. Vidal, C. Lopéz de Dicastillo, F. Rodriguez, A. Guarda, R. M. S. Cruz, M. J. Galotto, *J. Appl. Polym. Sci.* **2019**, *136*, 47090.
[10] P. Karuppuswamy, J. R. Venugopal, B. Navaneethan, A. L. Laiva, S. Sridhar, S. Ramakrishna, *Appl. Surf. Sci.* **2014**, *322*, 162.
[11] A. Ranga, M. P. Lutolf, J. Hilborn, D. A. Ossipov, *Biomacromolecules* **2016**, *17*, 1553.
[12] M. M. Fares, E. Shirzaei Sani, R. Portillo Lara, R. B. Oliveira, A. Khademhosseini, N. Annabi, *Biomater. Sci.* **2018**, *6*, 2938.
[13] J. Liu, H. Chen, Y. Wang, G. Li, Z. Zheng, D. L. Kaplan, X. Wang, X. Wang, *ACS Biomater. Sci. Eng.* **2020**, *6*, 1641.
[14] N. Gjorevski, M. P. Lutolf, *Nat. Protoc.* **2017**, *12*, 2263.
[15] F. Dini, G. Barsotti, D. Puppi, A. Coli, A. Briganti, E. Giannessi, V. Miragliotta, C. Mota, A. Pirosa, M. R. Stornelli, P. Gabellieri, F. Carlucci, F. Chiellini, *J. Bioact. Compat. Polym.* **2015**, *31*, 15.
[16] E. D. Boland, J. A. Matthews, K. J. Pawlowski, D. G. Simpson, G. E. Wnek, G. L. Bowlin, *Front. Biosci.* **2004**, *9*, 1422.
[17] L. Huang, K. Nagapudi, P. R. Apkarian, E. L. Chaikof, *J. Biomater. Sci., Polym. Ed.* **2001**, *12*, 979.
[18] A. M. Abdel-Mohsen, D. Pavlinak, M. Cilekova, P. Lepcio, R. M. Abdel-Rahman, J. Jancar, *Int. J. Biol. Macromol.* **2019**, *139*, 730.
[19] D. W. Urry, A. Pattanaik, X. Jie, T. Cooper Woods, D. T. McPherson, T. M. Parker, *J. Biomater. Sci., Polym. Ed.* **1998**, *9*, 1015.
[20] J. B. Leach, J. B. Wolinsky, P. J. Stone, J. Y. Wong, *Acta Biomater.* **2005**, *1*, 155.
[21] M. A. Nazeer, E. Yilgor, I. Yilgor, *Polymer* **2019**, *168*, 86.
[22] Y. Xu, L. Luo, B. Chen, Y. Fu, *Frontiers of Biol. in China* **2009**, *4*, 385.
[23] E. Adomavičiūtė, J. Baltušnikaitė-Guzaitienė, V. Juškaitė, M. Žilius, V. Briedis, S. Stanys, *J. Textile Inst.* **2017**, *109*, 278.
[24] E. Adomavičiūtė, S. Pupkevičiūtė, V. Juškaitė, M. Žilius, S. Stanys, A. Pavilonis, V. Briedis, *J. Nanomater.* **2017**, *1*, 2017.
[25] E. L. Ghisalberti, *Bee World* **2015**, *60*, 59.
[26] R. Bilginer, A. Arslan Yildiz, *Mater. Lett.* **2020**, *276*, 128191.
[27] F. H. Zulkifli, F. S. Jahir Hussain, M. S. B. Abdull Rasad, M. Mohd Yusoff, *Polym. Degrad. Stab.* **2014**, *110*, 473.
[28] R. H. Schmedlen, K. S. Masters, J. L. West, *Biomaterials* **2002**, *23*, 4325.
[29] S. Bonakdar, S. H. Emami, M. A. Shokrgozar, A. Farhadi, S. A. H. Ahmadi, A. Amanzadeh, *Mater. Sci. Eng., C* **2010**, *30*, 636.
[30] A. S. Asran, K. Razghandi, N. Aggarwal, G. H. Michler, T. Groth, *Biomacromolecules* **2010**, *11*, 3413.
[31] M. Zolghadri, S. Saber-Samandari, S. Ahmadi, K. Alamara, *Bull. Mater. Sci.* **2019**, *42*, 35.
[32] S. Mombini, J. Mohammadnejad, B. Bakhshandeh, A. Narmani, J. Nourmohammadi, S. Vahdat, S. Zirak, *Int. J. Biol. Macromol.* **2019**, *140*, 278.
[33] L. Peng, Y. Zhou, W. Lu, W. Zhu, Y. Li, K. Chen, G. Zhang, J. Xu, Z. Deng, D. Wang, *BMC Musculoskeletal Dis.* **2019**, *20*, 257.
[34] P. Liu, W. Chen, C. Liu, M. Tian, P. Liu, *Sci. Rep.* **2019**, *9*, 9534.
[35] X. Wang, T. Yucel, Q. Lu, X. Hu, D. L. Kaplan, *Biomaterials* **2010**, *31*, 1025.
[36] X.-L. Wang, I.-K. Oh, S. Lee, *Sens. Actuators, B* **2010**, *150*, 57.
[37] M. Ye, P. Mohanty, G. Ghosh, *Mater. Sci. Eng., C* **2014**, *42*, 289.
[38] B. Singh, L. Pal, *J. Mech. Behav. Biomed. Mater.* **2012**, *9*, 9.
[39] K. C. S. Figueiredo, T. L. M. Alves, C. P. Borges, *J. Appl. Polym. Sci.* **2009**, *111*, 3074.
[40] P. Sensharma, G. Madhumathi, R. D. Jayant, A. K. Jaiswal, *Mater. Sci. Eng. C Mater. Biol. Appl.* **2017**, *77*, 1302.
[41] C. Asawahame, K. Sutjarittangtham, S. Eitssayeam, Y. Tragoolpua, B. Sirithunyalug, J. Sirithunyalug, *AAPS PharmSciTech* **2015**, *16*, 182.
[42] J. I. Kim, H. R. Pant, H. J. Sim, K. M. Lee, C. S. Kim, *Mater. Sci. Eng. C Mater. Biol. Appl.* **2014**, *44*, 52.
[43] L. Wu, X. Yuan, J. Sheng, *J. Membr. Sci.* **2005**, *250*, 167.
[44] C. N. Grover, J. H. Gwynne, N. Pugh, S. Hamaia, R. W. Farndale, S. M. Best, R. E. Cameron, *Acta Biomater.* **2012**, *8*, 3080.
[45] S. K. Jaganathan, M. P. Mani, A. F. Ismail, P. Prabhakaran, G. Nageswaran, *Polym. Compos.* **2019**, *40*, 2039.
[46] K. Sutjarittangtham, S. Sanpa, T. Tunkasiri, P. Chantawannakul, U. Intatha, S. Eitssayeam, *J. Apicultural Res.* **2015**, *53*, 109.
[47] A. Masek, *Int. J. Electrochem. Sci.* **2019**, *14*, 1231.
[48] F. Zeighampour, F. Alihosseni, M. Morshed, *J. App. Poly. Sci.* **2018**, *135*, 45794.
[49] T. Wu, J. Sha, Y. Peng, X. Chen, L. Xie, Y. Ma, L.-S. Turng, *RSC Adv.* **2016**, *6*, 101660.
[50] S. Surucu, H. Turkoglu Sasmazel, *Int. J. Biol. Macromol.* **2016**, *92*, 321.
[51] G. A. Burdock, *Food Chem. Toxicol.* **1998**, *36*, 347.

How to cite this article: Bilginer R, Ozkendir-Inanc D, Yildiz UH, Arslan-Yildiz A. Biocomposite scaffolds for 3D cell culture: Propolis enriched polyvinyl alcohol nanofibers favoring cell adhesion. *J Appl Polym Sci*. 2021;138:e50287. https://doi.org/10.1002/app.50287